

# Controllable Prompt Tuning For Balancing Group Distributional Robustness

Hoang Phan Andrew Gordon Wilson Qi Lei

New York University

{hvp2011@, andrewgw@cims., ql518@}nyu.edu

March 6, 2024

## Abstract

Models trained on data composed of different groups or domains can suffer from severe performance degradation under distribution shifts. While recent methods have largely focused on optimizing the worst-group objective, this often comes at the expense of good performance on other groups. To address this problem, we introduce an optimization scheme to achieve good performance across groups and find a good solution for all without severely sacrificing performance on any of them. However, directly applying such optimization involves updating the parameters of the entire network, making it both computationally expensive and challenging. Thus, we introduce Controllable Prompt Tuning (CPT), which couples our approach with prompt-tuning techniques. On spurious correlation benchmarks, our procedures achieve state-of-the-art results across both transformer and non-transformer architectures, as well as unimodal and multimodal data, while requiring only 0.4% tunable parameters.

## 1 Introduction

Spurious correlation or shortcut learning arises when a classifier relies on non-predictive features that coincidentally correlate with class labels among training samples. For example, a *majority* of waterbirds are often found near water, while landbirds mostly appear near land. Even when being provided with a small number of *minority group examples*, such as waterbirds on land, or landbirds on water, model predictions are often still dominated by spurious features, in this case, the background, ignoring the salient feature, the foreground [68].

A variety of approaches aim to improve worst group performance, by oversampling high-loss samples [53, 90], undersampling the majority group [69] or re-training a last layer on group-balanced validation data [42]. A particularly popular and effective baseline, *Group Distributionally Robust Optimization* (GroupDRO) [68, 69], directly minimizes an estimated upper bound on worst group loss. However, all these procedures generally neglect knowledge transfer between groups. Moreover, high-error samples can potentially include noisy-label data that could hurt the model’s predictive ability if we try to learn them exhaustively [61]. Besides, DRO-based methods, in particular, are susceptible to overfitting, wherein their test performances can decline to the same as ERM with sufficiently long training [31, 64, 88].

To visually illustrate these limitations, we plot in Figure 1 the performance of a ResNet50 on the Waterbirds benchmark, trained with ERM, GroupDRO, and our approach (to be explained later). The plots demonstrate that while GroupDRO can improve the performance of the minority group (green line) early in training compared to ERM, it rapidly overfits and fails to maintain this performance over time. After training for ten epochs, the test performance gap between the

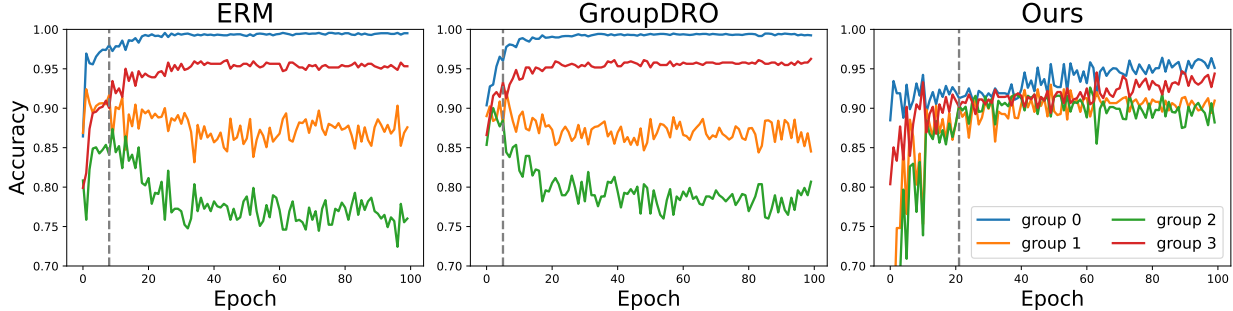


Figure 1: Accuracy curves on Waterbirds for four groups during training. Vertical lines indicate early stopping epochs when models perform best on the validation set.

minority and majority (blue line) groups grows sharply. To address these critical limitations, we introduce a systematic approach to train a model that exhibits consistently high performance across all groups. Specifically, at each iteration, we identify a descending direction that benefits the groups simultaneously rather than focusing on an individual group. Figure 1 shows that our proposed method performs almost equally well in every group, thanks to our balancing mechanism.

Moreover, we aim to control the group-wise learning process by ensuring that the magnitude of loss for different groups is inversely proportional to a predefined vector  $\mathbf{c}$ . Varying this hyperparameter  $\mathbf{c}$  adjusts the trade-off between the worst group and the average performance, yielding a more flexible method than prior work that only focuses on maximizing the worst group accuracy. However, computation can grow linearly with the number of controlling vectors  $\mathbf{c}$ . To overcome this challenge, we propose decoupling our optimization framework with parameter-efficient fine-tuning (PEFT) techniques that considerably reduce the number of trainable parameters. With the model compression ability powered by prompt-tuning, our proposed model can scale well for a large number of controlling vectors with a small parameter increase, e.g., 0.01% and 0.003% per value of  $\mathbf{c}$  for Vision Transformer [23] and CLIP [66], respectively.

**Contribution.** In this work, we introduce **CPT**, a **C**ontrollable **P**rompt **T**uning method to prevent models from learning spurious features. In summary, our key contributions are depicted as follows:

- Drawing inspiration from the principles of multi-objective optimization theory, we introduce a novel balancing mechanism to address the challenges of group distributional robustness. Our method not only considers the worst group but also leverages the gradient information from all groups to determine an ultimate updating direction that benefits all of them.
- While the above rigid balancing procedure works well in different scenarios, we extend our method by introducing a controlling vector that allows us to dynamically adjust the priority across groups. Additionally, we integrate prompt tuning techniques to enhance the scalability of our method as the complexity and number of controlling vectors increase and to make it applicable for de-biasing large transformers-based models.
- We conduct intensive experiments on many different benchmarks, where CPT consistently exhibits superior performance. Our method surpasses the current state-of-the-art baselines on Waterbirds and CelebA datasets while updating 0.4% parameters. Moreover, it also

outperforms recently proposed methods that aim to de-bias Vision Transformer and CLIP models with minimal training cost.

## 2 Related work

We first review relevant methods to enhance distributional robustness and then discuss prior work related to the two essential parts of our proposed method: transformer and parameter-efficient fine-tuning.

**Distributional robustness** can be compromised for reasons like selection bias or spurious correlation across tasks. For selection bias on individual samples, prior works seek to reduce bias via practices like importance reweighting [36, 72, 16, 46], hard sample reweighting [53, 60] or distribution matching and discrepancy minimization [17, 7, 8, 63], and domain-adversarial algorithms [27, 58] across tasks in their feature representation space. For selection bias on groups or subpopulation, namely subpopulation shift or dataset imbalance, label propagation [11, 8] or other consistency regularization [59, 84] are used to generalize the prediction to broader domains. In particular, GroupDRO [68, 69] or other relevant methods [44, 39] select descending direction more in favor of the worse performing/minority group(s) during training.

Improving distributional robustness also requires mitigating the effect of environmental features. Prior work uses model ensemble [45] or model soups [81] to learn rich features and reduce the effect of spurious features. More practices include invariant feature representation learning [6, 14], domain generalization [44, 73, 71] or through data augmentation [83, 86].

**Transformer** In the past few years, transformer [77] has emerged as a dominant architecture for a wide range of applications, exhibiting their profound capacity in modeling different modalities: languages [21, 55, 76], vision [23, 12], speech [67, 79], and time series [49, 30]. Due to its ability to process multiple modalities, transformer-based architectures were widely adopted for image understanding using different types of supervision. For example, Vision Transformer (ViT) [23] utilizes masked patches for pre-training and image-label supervision for fine-tuning. Notably, Contrastive Language-Image Pre-training (CLIP) [66], which was pre-trained on billion-scale image-text pairs, has demonstrated excellent zero-shot performance in image classification tasks. Despite obtaining impressive results on various downstream tasks, over-parameterization is still a crucial problem for transformer [26, 62] which potentially causes overfitting [48] and unintended biases [1, 80, 24, 89] more severely than small-scale architectures [69].

**Parameter-Efficient Fine-Tuning** While conventional training updates the entire network, prior work has shown that it is possible to achieve performance comparable with full fine-tuning by instead updating a small set of parameters [51, 33, 34]. Early work in this line of research includes adapter [37, 13, 74], which adds a lightweight fully connected network between the layers of a frozen pre-trained model. Since then, there have been many other methods that update subsets of the network [32, 28, 87] or reparametrize the weights of the network using low-rank decompositions [2, 38, 25]. Another appealing PEFT strategy is prompt tuning, which prepends a few trainable tokens before the input sequence or hidden state to encode task-specific knowledge to the pre-trained model [47, 50, 94, 40].

### 3 Background

In this section, we first formulate the problem of group robustness and recap the technical details of GroupDRO, then revisit some concepts of multi-objective optimization.

#### 3.1 Problem formulation

Formally, we consider the conventional setting of classifying an input  $x \in \mathcal{X}$  as a target  $y \in \mathcal{Y}$ , where  $\mathcal{X}, \mathcal{Y}$  are input and label spaces, respectively. We are given a training dataset composed of  $K$  groups from the set  $\mathcal{G}$ , where each group  $g \in \mathcal{G}$  consists of  $n_g$  instances sampled from the probability distribution  $P_g(\mathcal{X}, \mathcal{Y})$ . Since the numbers of examples are different among groups in the training data, we consider groups with relatively large  $n_g$  as majority groups and those with small  $n_g$  as minority groups. Our main goal is to develop a model that performs effectively across all groups within  $\mathcal{G}$  to avoid learning spurious correlations.

Following previous methods [69], we adopt two metrics: worst group accuracy, indicating the minimum test accuracy across all groups  $g \in \mathcal{G}$ , and average accuracy, which represents the weighted average test accuracy with the weights corresponding to the relative proportions of each group in the training data. It is worth noting that commonly used datasets for group robustness often exhibit skewed training set distributions, the weighted average score is thus dominated by the performance of the model on groups that include large numbers of training data. Therefore, we propose to evaluate the model performance by additionally reporting the mean (unweighted average) accuracy score across different groups.

#### 3.2 Group distributionally robust optimization

GroupDRO learns the model parameters  $\theta$  by directly optimizing for the worst-group training loss as follows:

$$\max_{g \in \mathcal{G}} \mathbb{E}_{(x,y) \sim P_g(\mathcal{X}, \mathcal{Y})} [\ell(f_\theta(x), y)]$$

for some loss function  $\ell : \mathcal{Y} \times \mathcal{Y} \rightarrow \mathbb{R}^+$ . Then, their updating formula at each step is given by:

$$g^* = \arg \max \ell_g(\theta) \quad \text{and} \quad \theta^{t+1} = \theta^t - \eta \nabla_{\theta} \ell_{g^*}, \quad \text{where } \eta \text{ is the learning rate.}$$

#### 3.3 Multi-objective Optimization

Assume that we are given  $m$  objectives functions  $f_i(x)$ ,  $i \in [m]$  where  $x \in \mathbb{R}^d$  and each  $f_i : \mathbb{R}^d \rightarrow \mathbb{R}$  is a scalar-valued function (we use the  $[m]$  notation to denote the set  $\{1, 2, \dots, m\}$ ). In the multi-objective optimization (MOO) problem, we are interested in minimizing a vector-valued objective function whose  $i$ -th component is  $f_i(x)$ :

$$\vec{F}(x) = [f_1(x), f_2(x), \dots, f_m(x)] \tag{1}$$

In general, an optimal solution for this objective vector function does not exist since each of the individual function  $f_i(x)$  does not necessarily guarantee to have the same minimum solution. Alternatively, we expect to obtain a solution, from which we cannot improve any specific objective without hurting another. According to the above formulation, the solution [95] of the multi-objective minimization problem is formally defined as follows:

**Definition 1.** (Pareto dominance) Let  $x_1, x_2$  be two solutions for the multi-objective optimization problem in Equation 1,  $x_1$  dominates  $x_2$  ( $x_1 \prec x_2$ ) if and only if  $f_i(x_1) \leq f_i(x_2) \forall i \in [m]$  and  $\exists j \in [m]$  s.t.  $f_j(x_1) < f_j(x_2)$ .

**Definition 2.** (Pareto optimality) A solution  $x^*$  in problem 1 is said to be Pareto optimal if it is not dominated by any other solution. Therefore, the solutions set of the multi-objective minimization problem is given by  $\mathcal{P} := \{x \mid \nexists x' : x' \prec x\}$ . This set of all Pareto optimal solutions is called the Pareto set while the collection of their images in the objective space is called the Pareto front.

**Gradient-based MOO** Désidéri [20] shows that the descent direction can be found in the convex hull composed of gradients corresponding to different objectives  $\{\mathbf{h}^i := \nabla f_i\}_{i=1}^m$ :

$$\mathcal{CH} = \left\{ \mathbf{H}^\top \boldsymbol{\alpha} = \sum_{i=1}^m \alpha_i \mathbf{h}^i \mid \boldsymbol{\alpha} \in \Delta_m \right\}$$

where  $\Delta_m$  denotes the  $m - 1$  dimension simplex.

Moreover, they introduce the Multiple Gradient Descent Algorithm (MGDA), which calculates the minimum-norm gradient vector  $\mathbf{h}$  that lies in the convex hull:  $\mathbf{h} = \operatorname{argmin}_{\mathbf{h} \in \mathcal{CH}} \|\mathbf{h}\|_2$ . This approach can guarantee that the obtained solutions lie on the Pareto front, from which we cannot find an updating direction that decreases all objectives simultaneously.

## 4 Proposed method

In GroupDRO, the updating formula solely focuses on the worst-performing group, which is susceptible to challenges when groups exhibit varying loss magnitude, noise, and transfer characteristics. For example, among the high-loss group, there might exist a few outliers that have large input shifts or even wrong labels, which can raise the training loss of the whole group and prevent the model from fitting other groups.

### 4.1 Balancing group distributional robustness

In this paper, we go beyond the worst group approach of GroupDRO to examine all groups at a time. To encourage the model to learn from different groups at each step to avoid struggling on just the hardest one only, we propose to minimize the following  $K$ -dimension loss vector:

$$\vec{\mathcal{L}}(\theta) = \left\{ \mathbb{E}_{(x,y) \sim P_{g^k}(\mathcal{X}, \mathcal{Y})} [\ell(f_\theta(x), y)] \right\}_{k=1}^K \quad (2)$$

where  $K$  is the number of groups and  $g^k$  is the  $k$ -th group.

At  $t$ -th iteration, we search for an update vector that minimizes the weighted sum of group losses:

$$d_t(w) = w^\top \nabla \vec{\mathcal{L}}(\theta_t) = \sum_{k=1}^K w_k \nabla \ell_k(\theta_t) \quad (3)$$

Then, the updating formula of our algorithm is then given by  $\theta_{t+1} = \theta_t - \eta d_t(w)$  for some step size  $\eta \in \mathbb{R}^+$ . The coefficient  $w$  is chosen such that our update rule can benefit all groups  $d_t(w)^\top \nabla \ell_k(\theta_t) \geq 0$ . To this end, a straightforward approach that is readily applicable to optimize

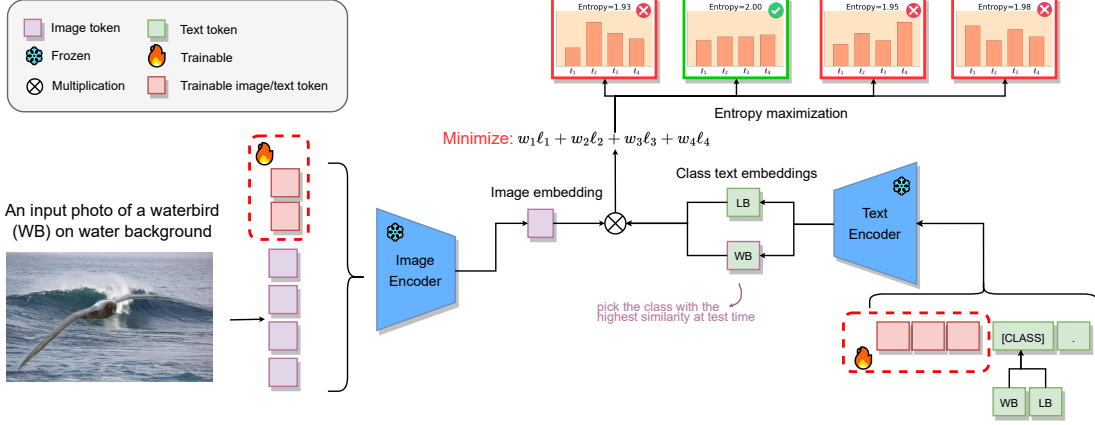


Figure 2: Overview of our method on the Waterbirds dataset. Our main objective is not only to improve model performance across groups by optimizing their loss functions  $\ell_1, \ell_2, \ell_3, \ell_4$ , but also to maximize the entropy over this loss distribution.

the objective (2) is applying MGDA to find the solution of (3) that yields the minimum Euclidean norm of the composite gradient:

$$d_t^* = \arg \min_{w \in \Delta_K} \left\| \sum_{k=1}^K w_k \nabla \ell_k(\theta_t) \right\|_2 \quad (4)$$

However, MGDA is often biased toward objectives with smaller gradient magnitudes [54], and lacks controllable property (i.e. could not adjust the group that we want to focus more or less at each update), which can be utilized to balance the loss between groups. Hence, we introduce a new objective that steers the updating direction to obtain our desired balanced magnitude among groups. Assuming that the entropy  $H(p)$  measures the diversity of a continuous distribution  $p$ , this behavior could be achieved via maximization of the entropy with respect to the distribution of loss functions:

$$\mathcal{L}_{ent}(\theta) = H(\text{softmax}(\vec{\mathcal{L}}(\theta))) = H\left(\text{softmax}\left(\{\mathbb{E}_{P_{g^k}}[\ell(f_\theta(x), y)]\}_{k=1}^K\right)\right) \quad (5)$$

**Theorem 3.** Assume that the loss function  $\ell$  is differentiable up to the first order with respect to  $\theta$ , then following

$$d_{ent} := \sum_{i=1}^K \nabla \ell_i(\theta) \left[ p_i \log(p_i) - p_i \sum_{j=1}^K \log(p_j) p_j \right]$$

where  $p_i = \frac{e^{\ell_i(\theta)}}{\sum_{j=1}^K e^{\ell_j(\theta)}}$ , maximizes the objective  $\mathcal{L}_{ent}(\theta)$ .

The proof of Theorem 3 is deferred to Appendix A. Theorem 3 provides us with the updating rule that increases the entropy term in Equation (5) the most. To balance the learning across groups, we seek the coefficient  $w$  that maximizes the cosine similarity with  $d_{ent}$  and does not conflict against the gradient vector of each group. Denotes  $w'_i = p_i \log(p_i) - p_i \sum_{j=1}^K \log(p_j) p_j$ , this is equivalent to optimizing:

$$\begin{aligned} w^* &= \arg \max_{w \in \Delta_K} d_t(w)^\top d_{ent} \\ \text{s.t. } & d_t(w)^\top \nabla \ell_k(\theta_t) \geq 0 \quad \forall k \in [K]. \end{aligned} \quad (6)$$

While the balance between loss magnitude is not achieved, we strictly follow the updating direction that decreases training errors of high-loss groups but slightly relaxes constraints in the optimization problem (6) to allow bounded increases among groups that already have small loss magnitudes.

$$\begin{aligned}
w^* &= \arg \max_{w \in \Delta_K} d_t(w)^\top d_{ent} \\
&= \arg \max_{w \in \Delta_K} w^\top \nabla \vec{\mathcal{L}}(\theta)^\top \nabla \vec{\mathcal{L}}(\theta) w' \\
\text{s.t. } &\forall k \in [K]: \\
&d_t(w)^\top \nabla \ell_k(\theta_t) \geq 0 \text{ if } \ell_k(\theta_t) = \max_{k \in [K]} \ell_k(\theta_t). \\
&d_t(w)^\top \nabla \ell_k(\theta_t) \geq d_{ent}^\top \nabla \ell_k(\theta_t) \text{ if } \ell_k(\theta_t) < \max_{k \in [K]} \ell_k(\theta_t).
\end{aligned} \tag{7}$$

The second constraint guarantees that the obtained solution is not worse than  $d_{ent}$  on those groups in which the model is performing well or when  $d_{ent}$  itself intrinsically supports learning them. Once the loss magnitude is almost balanced ( $\|d_{ent}\| \leq \epsilon$ ), we simply update the model parameter by the average group gradients, i.e.  $w = (\frac{1}{K}, \frac{1}{K}, \dots, \frac{1}{K})$ .

In summary, the key difference between our proposed method and GroupDRO is that we solve a small  $K$ -dimensional optimization problem to find the updating direction that not only focuses on the worst group but also improves the performance in other groups and balances the loss magnitude between them at the same time. In practical settings, the group number  $K$  is often a small number (e.g.  $K = 4$ ), thus could be efficiently solved using standard linear programming libraries [22, 5] without introducing significant computational overhead (Appendix B).

## 4.2 Controllable prompt tuning for balancing group distributional robustness

To achieve the controllable property, we apply the optimization procedure in section 4.1 on  $\ell_k(\theta) = c_k \mathbb{E}_{P_{g^k}} [\ell(f_\theta(x), y)]$  where  $\mathbf{c} \in \mathbb{R}^K$  is a pre-defined vector that is used to adjust the magnitude of group losses. Intuitively, the principle behind our proposed objective is to enforce the loss vector  $\vec{\mathcal{L}}(\theta)$  to be inversely proportional to  $\mathbf{c}$ , from which we can adjust the group loss magnitude, and thus control the trade-off between them by varying  $\mathbf{c}$ . For example, we can put more weight on penalizing loss terms of some specific groups to accelerate the learning progress on those groups, or conversely slow down the learning to avoid overfitting on oversampled groups [19].

In practice, tuning the value of  $\mathbf{c}$  to obtain our desired model behavior requires learning multiple models individually and independently. Therefore, the computational complexity of our proposed method can grow linearly with the number of vectors  $\mathbf{c}$ , thus being very expensive in the context of deep learning. To reduce overhead, we adopt the usual practice of parameter-efficient fine-tuning methods and optimize only a small portion of the model. In particular, we freeze the main backbone while introducing lightweight prompt sets, one for each task. For example, we employ the same ViT backbone for the two datasets Waterbirds, CelebA, but using different sets of prompts (Section 5).

**Overview of our proposed method** is depicted in Figure 2, given an input image belonging to one of a group  $\{g^1, g^2, \dots, g^K\}$  and a set of classes, we solve the optimization problem (7) to find the reweighting coefficient  $w$  that maximizes the entropy  $\mathcal{L}_{ent}(\theta)$  while reasonably decreases group losses. While Figure 2 illustrates our proposed method on the CLIP model on the image classification task, it applies to other transformer-based models and task types. In our experiment,

we exploit both image-end prompts and language-end prompts tuning on frozen ViT and CLIP backbones, respectively.

**Prompt tuning for Vision Transformer:** Regarding the prompt design for a ViT of  $N$  layers, we use the set of continuous learnable tokens  $\{\mathbf{P}_n\}_{n=0}^{N-1}$ . Each  $\mathbf{P}_n \in \mathbb{R}^{L \times D}$ , where  $D, L \in \mathbb{N}$  indicate the prompt length and latent space dimension, respectively. Subsequently, the input at the  $(n+1)$ -th layer follows the format of  $[x_n, \mathbf{P}_n, \mathbf{E}_n]$ , where  $\mathbf{x}_n, \mathbf{E}_n \in \mathbb{R}^D$  represent the [CLASS] token and image patch embeddings after  $n$ -th layer while  $[\cdot, \cdot]$  denotes the concatenation operator. Thus, the number of trainable parameters for this image-end prompt set is  $L \times N \times D$ .

**Prompt tuning for CLIP:** Being trained on an enormous amount of image-text pairs, CLIP offers an expressive representation for both language and image inputs by using two separate encoders, one for each modality, as shown in Figure 2. Since the image encoder can be either ResNet [35], ConvNeXt [57] or ViT [23], we conduct prompt tuning on the transformer text encoder for consistency. In short, we employ a learnable context prompt of length  $L$ :  $\mathbf{P} \in \mathbb{R}^{L \times D}$ , to replace the hand-crafted prompt used by the original CLIP (i.e., "this is a photo of a "). Based on this design, the input for the text encoder of each class has the format of  $[x, \mathbf{P}]$ , where  $x$  is the [CLASS] embedding of the corresponding class name and has the same dimension of  $D$ . These learnable tokens  $\mathbf{P}$  are better at capturing domains-specific knowledge than those artificial prompt [92, 93] and can be learned to de-bias the original CLIP model while introducing a few trainable parameters ( $N \times D$ ).

## 5 Experiments

In this section, we evaluate the effectiveness of the proposed CPT method on benchmark image datasets in the presence of spurious features: Waterbirds [68], CelebA [56], MetaShift [52] and ISIC [15]. Due to the space limit constraint, we briefly provide an overview of our experimental setup below, see Appendix B for more details and additional results.

### 5.1 Datasets

**Waterbirds** is created by placing bird photos from the Caltech-UCSD Birds dataset [78] with background images taken from Places [91]. The target attributes are foreground objects (i.e. landbird or waterbird) while spurious correlations are background (i.e. land or water landscape).

**CelebA** is a factual dataset containing 200K face images of celebrities. The goal is to classify blond/non-blond hair color. Statistically, more than 94% of blond hair examples in the training set are women.

**MetaShift** is another real-world dataset [52] for cat-dog classification, where the cat and dog images are spuriously correlated with indoor (e.g. bed) and outdoor objects (e.g. bike). For evaluation, models are given dog and cat images associated with shelf background, which does not appear in the training set. Thus, this dataset represents a more coherent distributional shift, compared to other benchmarks.

**ISIC** is an even more challenging dataset with the appearance of multiple spurious features [15], which includes dermoscopic images of skin lesions with target attributes benign or melanoma. Visual examples of those datasets, along with the size for each group in train, validation, and test sets are given in Appendix B.



## 5.2 Baselines

Following the previous studies, we compare CPT against other state-of-the-art methods for mitigating spurious correlations, including GroupDRO [68], Deep Feature Reweighting (DFR) [42], Progressive Data Expansion (PDE) [19], Subsample [19], Common Gradient Descent (CGD) [64] with the access to the group information during training. Besides, we consider those methods require group labels for validation: Learning from failure (LfF) [60], Just Train Twice (JTT) [53], Predictive Group Invariance (PGI) [3], Contrastive Input Morphing (CIM) [75], Correct-n-Contrast (CNC) [90], or those do not use group annotations at all like Empirical Risk Minimization (ERM) and Automatic Feature Reweighting (AFR) [65]. Moreover, we also report the results from two recent studies of spurious correlation on ViT [29] and CLIP [85].

Regarding the baselines for those experiments further taking the distribution shift into account, we follow exactly the protocol of [82] and compare our method to Empirical Risk Minimization (ERM), Upweighting (UW), Invariant risk minimization (IRM) [6], Information Bottleneck based Invariant Risk Minimization (IB-IRM) [4], Variance Risk Extrapolation (V-REx) [44], CORrelation ALignment (CORAL) [73], and Fish [71]; instance reweighting methods: GroupDRO [68], JTT [53], Domain mixup (DM-ADA) [83], Selective Augmentation (LISA) [86] and the current state-of-the-art method on those benchmarks Discover and Cure (DISC) [82].

## 5.3 Model training and evaluation

We examine our proposed method on ResNet50 [35], ViT-B/16 [23] and different variants of OpenAI’s CLIP [66] to align with previous work [42, 29, 85]. For prompt tuning on ViT, we employ prompts of lengths  $L = 5$  in the MetaShift and ISIC, or  $L = 10$  in the Waterbirds and CelebA datasets. Similarly,  $L$  is set to 16 for all CLIP backbones throughout our experiment. Unless otherwise explicitly mentioned in the experiment, the value of the controlling vector  $c$  is set to the default value of  $(1, \dots, 1)$ . Other detailed configurations are relegated to Appendix B.

Due to the large number of groups in ISIC, we calculate the AUROC score [10], following [82, 9] while computing average, worst-group and mean (if possible) accuracy scores for other datasets. For a fair and precise comparison, results of baselines are taken from recent studies [19, 82, 64, 90, 41] and reported directly from original papers.

## 5.4 Results

**Waterbirds and CelebA** We start by validating CPT on two well-established benchmarks for investigating spurious correlation, namely Waterbirds and CelebA in Table 1. From the results, we see that CPT consistently achieves the best worst-group accuracy compared with the recent state-of-the-art methods such as DFR and PDE on both datasets. Remarkably, our method only updates a tiny portion (0.4%) of parameters. As such, CPT is much more computationally efficient than methods that need to update the entire network. Furthermore, we see that CPT has strong gains in average accuracy, thus not only outperforming other spurious correlation methods on both metrics but also closing the gap to the average accuracy of ERM. Another interesting observation is that those baselines aim to balance the learning between groups via downsampling the minority groups (Subsample), reweighting group losses inversely proportional to the group populations (UW), or computing scaling weights using group training performance to upweight the worst-group loss (GroupDRO), are effective in alleviating spurious correlation. Even though, CPT still exhibits

Table 1: Overall results on Waterbirds and CelebA datasets with best methods are highlighted in **bold**. Performance is evaluated on the test set with models early stopped at the highest worst-group accuracy on the validation set.

Method	Train group info	Validation group info	Train once	Waterbirds			CelebA		
				Worst	Average	# Params	Worst	Average	# Params
ERM	×	×	✓	70.0 $\pm$ 2.3	97.1 $\pm$ 0.1	23M	45.0 $\pm$ 1.5	94.8 $\pm$ 0.2	23M
AFR	×	×	×	90.4 $\pm$ 1.1	94.2 $\pm$ 1.2	23M	82.0 $\pm$ 0.5	91.3 $\pm$ 0.3	23M
LfF	×	✓	×	78.0 $N/A$	91.2 $N/A$	23M	77.2 $N/A$	85.1 $N/A$	23M
SSA	×	✓	×	89.0 $\pm$ 0.6	92.2 $\pm$ 0.9	23M	89.8 $\pm$ 1.3	92.8 $\pm$ 1.3	23M
JTT	×	✓	×	86.7 $N/A$	93.3 $N/A$	23M	81.1 $N/A$	88.0 $N/A$	23M
PGI	×	✓	×	79.5 $\pm$ 1.9	95.5 $\pm$ 0.8	23M	85.3 $\pm$ 0.3	87.3 $\pm$ 0.1	23M
CIM	×	✓	×	77.2 $N/A$	95.6 $N/A$	23M	83.6 $N/A$	90.6 $N/A$	23M
CnC	×	✓	×	88.5 $\pm$ 0.3	90.9 $\pm$ 0.1	23M	88.9 $\pm$ 1.3	88.9 $\pm$ 0.5	23M
DFR	×	✓	×	92.9 $\pm$ 0.2	94.2 $\pm$ 0.4	23M	88.3 $\pm$ 1.1	91.3 $\pm$ 0.3	23M
UW	✓	✓	✓	88.0 $\pm$ 1.3	95.1 $\pm$ 0.3	23M	83.3 $\pm$ 2.8	92.9 $\pm$ 0.2	23M
Subsample	✓	✓	✓	86.9 $\pm$ 2.3	89.2 $\pm$ 1.2	23M	86.1 $\pm$ 1.9	91.3 $\pm$ 0.2	23M
LISA	✓	✓	×	89.2 $\pm$ 0.6	91.8 $\pm$ 0.3	23M	89.3 $\pm$ 1.1	92.4 $\pm$ 0.4	23M
GroupDRO	✓	✓	✓	86.7 $\pm$ 0.6	93.2 $\pm$ 0.5	23M	86.3 $\pm$ 1.1	92.9 $\pm$ 0.3	23M
CGD	✓	✓	✓	88.9 $\pm$ 0.8	91.3 $\pm$ 0.6	23M	90.0 $\pm$ 0.8	92.5 $\pm$ 0.2	23M
DISC	✓	✓	×	88.7 $\pm$ 0.4	93.8 $\pm$ 0.7	23M	N/A	N/A	N/A
PDE	✓	✓	✓	90.3 $\pm$ 0.3	92.4 $\pm$ 0.8	23M	91.0 $\pm$ 0.4	92.0 $\pm$ 0.6	23M
CPT	✓	✓	✓	<b>93.5<math>\pm</math>0.4</b>	96.3 $\pm$ 0.2	<b>94k</b>	<b>92.0<math>\pm</math>0.3</b>	93.2 $\pm$ 0.3	<b>94k</b>

impressive performance compared to the aforementioned methods by using an adaptive balancing mechanism at each iteration instead of relying on fixed reweighting coefficients.

**De-bias ViT and CLIP** Motivated by recent studies focusing on investigating spurious correlations of pre-trained transformer-based models [85, 18], we apply our proposed algorithm on ViT and CLIP and then compare them against those work. It is worth noting that, the authors did not experiment on CelebA with the blond hair target. Hence, we only show their original results on Waterbirds in Figure 3 and Table 2. As can be seen in Figure 3, while CPT enjoys much less computation and memory overhead (only 0.1% and 0.04% compared to ViT-B/16 itself and BiT-M-R50x3 [29]) it still outperforms the second-best model by a large margin. This significant improvement comes from our prompting design and optimization contribution, respectively. Details of backbones are given in Appendix B.

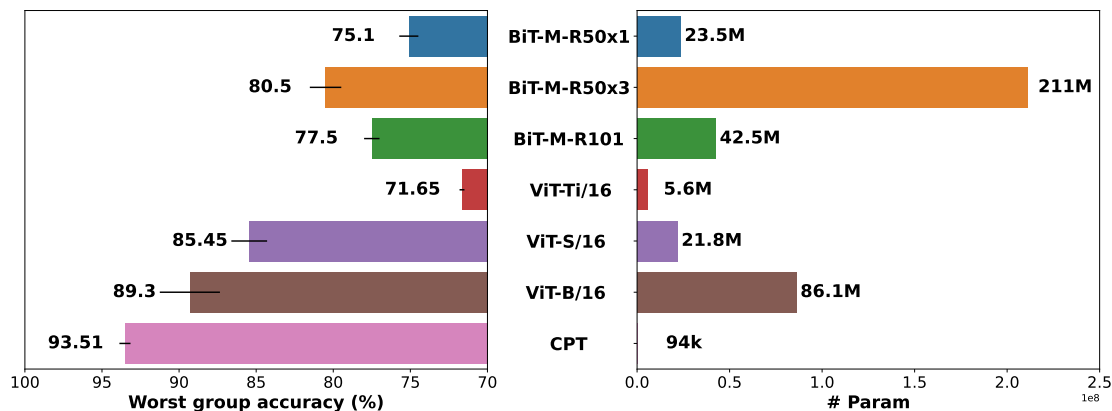


Figure 3: Results of fine-tuning ViT backbones on Waterbirds. Error bars represent the standard deviation over independent runs.

As shown in Table 2,  $\text{CPT}_{\text{balance}}$  (i.e. CPT with  $c = (1, \dots, 1)$ ) clearly outperforms all other alternatives using the same number of trainable parameters, which proves the effectiveness of our optimization framework. Furthermore, when varying the coefficient  $c$ , one can control the trade-off between group performance, yielding a much more flexible learning algorithm for group distributional robustness. Indeed, increasing coefficients of the majority groups (e.g.  $c = (2, 1, 1, 1.5)$  in this setting) helps improve the average accuracy of CPT to perform on par or better than Yang et al. [85] on both metrics while updating only 0.05% and 1% of the model parameters. Thus, this again suggests the clear efficiency advantage of our prompt tuning, which offers scalability for controlling adjustment. Since CPT has a larger capacity to control the learning between groups, we can sacrifice worst-group accuracy for the gain in performance on other groups (line 11) and vice-versa (line 10). Intriguingly, while obtaining impressive performance on CLIP-RN50, Contrastive Adapter [89] falls far behind other baselines on CLIP ViT-L/14@336px.

Table 2: Performance of CLIP models on Waterbirds. † indicates our implemented results. We use **Bold** font to indicate the best methods for different numbers of trainable parameters. N/A denotes those methods do not report the number of trainable parameters.

Model	ResNet50			ViT-L/14@336px		
	Average	Worst	# Params	Average	Worst	# Params
Pre-trained CLIP	90.8	44.9	0	88.5	34.0	0
Fine-tuned CLIP	81.3	77.1	14789632	97.2	89.7	786432
ERM	93.5	54.4	14789632	96.8	58.1	786432
ERM Adapter	96.0	63.0	524288	97.8	76.1	524288
Contrastive Adapter	88.2	82.5	263424	94.5	85.3	197632
DFR	91.8	63.9	N/A	96.1	65.9	N/A
FairerCLIP	84.3	75.4	N/A	92.2	86.0	N/A
GroupDRO	83.3	73.7	14789632	94.1	90.8	786432
Yang et al. [85]	83.2	77.5	14789632	96.9	90.5	786432
$\text{CPT}_{\text{balance}}$	85.8	<b>82.8</b>	14789632	94.0	<b>92.9</b>	786432
ERM†	85.7	64.6	8192	97.4	84.3	12288
GroupDRO†	81.0	76.7	8192	95.8	90.5	12288
CPT	83.3	78.4	8192	97.0	90.2	12288
$\text{CPT}_{\text{balance}}$	81.8	<b>79.8</b>	8192	95.6	<b>91.9</b>	12288

**MetaShift and ISIC** Results on those datasets are depicted in Table 3, along with the number of parameters required for each baseline. We mostly pick those that utilize group information during training for better benchmarking the efficiency of our proposed framework. In summary, the performance of CPT exceeds other methods by large margins, especially  $\approx 10$  AUROC score on ISIC. On MetaShift, it is also the best method in terms of average and worst-group accuracy, improving the performance by approximately 4%.

## 5.5 Ablation studies

In this section, we provide different ablation studies to see how each component in our proposed method individually contributes to the overall improvement of CPT.

Table 3: Experimental results on MetaShift and ISIC dataset.

Method	MetaShift		ISIC	# Params
	Average	Worst	AUROC	
ERM	72.9 $\pm$ 1.4	62.1 $\pm$ 4.8	36.4 $\pm$ 0.7	23M
UW	72.1 $\pm$ 0.9	60.5 $\pm$ 3.8	39.2 $\pm$ 0.6	23M
IRM	73.9 $\pm$ 0.8	64.7 $\pm$ 2.1	45.5 $\pm$ 3.6	23M
IB-IRM	74.8 $\pm$ 0.2	65.6 $\pm$ 1.1	38.6 $\pm$ 1.7	23M
V-REx	72.7 $\pm$ 1.7	60.8 $\pm$ 5.5	24.5 $\pm$ 6.4	23M
CORAL	73.6 $\pm$ 0.4	62.8 $\pm$ 2.7	37.9 $\pm$ 0.7	23M
Fish	64.4 $\pm$ 2.0	53.2 $\pm$ 4.5	42.0 $\pm$ 0.8	23M
GroupDRO	73.6 $\pm$ 2.1	66.0 $\pm$ 3.8	36.4 $\pm$ 0.9	23M
JTT	74.4 $\pm$ 0.6	64.6 $\pm$ 2.3	33.8 $\pm$ 0.0	23M
DM-ADA	74.0 $\pm$ 0.8	65.7 $\pm$ 1.4	35.8 $\pm$ 1.0	23M
LISA	70.0 $\pm$ 0.7	59.8 $\pm$ 2.3	38.0 $\pm$ 1.3	23M
DISC	75.5 $\pm$ 1.1	73.5 $\pm$ 1.4	55.1 $\pm$ 2.3	23M
CPT	<b>79.8<math>\pm</math>2.6</b>	<b>77.0<math>\pm</math>0.8</b>	<b>64.9<math>\pm</math>1.2</b>	<b>47k</b>

**Optimization and Backbones** Table 4 (rows 5 and 7) eliminates the entropy objective and uses the average gradient  $1/K \sum \nabla \ell_i(\theta)$  to update the model. While this strategy can improve mean accuracy among groups, compared to ERM, the performance has a significant drop compared to our optimization procedure. This conclusion suggests that conducting simple gradient averaging when there are still large differences among group losses could cause severe bias in training. On the other hand, there is no significant difference between the performance of fully fine-tuning ResNet50 (row 6) and prompt tuning on ViT-B/16 (row 8), which indicates that our method does not benefit much from more powerful backbones. Instead, we remind readers that prompting in CPT is introduced to scale up our proposed algorithm. Thus, even applying our proposed balancing method alone can boost the performance of ResNet to exceed GroupDRO by large margins on WaterBirds (5.2%) and CelebA (5.1%).

Table 4: Ablation results for different architectures and optimization procedures.

Dataset	Method	Average	Worst	# Params
MetaShift	ERM	72.9 $\pm$ 1.4	62.1 $\pm$ 4.8	23M
	GroupDRO	73.6 $\pm$ 2.1	66.0 $\pm$ 3.8	23M
	DISC	75.5 $\pm$ 1.1	73.5 $\pm$ 1.4	23M
	CPT <sub>w/o entropy</sub> (ResNet50)	76.1 $\pm$ 0.7	62.8 $\pm$ 1.8	23M
	CPT (ResNet50)	78.2 $\pm$ 2.5	76.9 $\pm$ 2.0	23M
	CPT <sub>w/o entropy</sub>	77.3 $\pm$ 0.8	74.7 $\pm$ 2.5	<b>47k</b>
	CPT	<b>79.8<math>\pm</math>2.6</b>	<b>77.0<math>\pm</math>0.8</b>	<b>47k</b>
Waterbirds	ERM	97.1 $\pm$ 0.1	70.0 $\pm$ 2.3	23M
	GroupDRO	93.2 $\pm$ 0.5	86.7 $\pm$ 0.6	23M
	CPT (ResNet50)	90.9 $\pm$ 0.2	91.9 $\pm$ 0.3	23M
	CPT	96.3 $\pm$ 0.2	<b>93.5<math>\pm</math>0.4</b>	<b>94k</b>
CelebA	ERM	94.8 $\pm$ 0.2	45.0 $\pm$ 1.5	23M
	GroupDRO	92.9 $\pm$ 0.3	86.3 $\pm$ 1.1	23M
	CPT (ResNet50)	92.7 $\pm$ 0.3	91.4 $\pm$ 0.8	23M
	CPT	93.2 $\pm$ 0.3	<b>92.0<math>\pm</math>0.3</b>	<b>94k</b>

Table 5: Performance on other CLIP variants, where CPT has the lowest gap between worst and average accuracy.

Model	Last layers ResNet101 13740544			Prompting ResNet101 8192			Last layer ViT-B/16 393216			Prompting ViT-B/16 8192		
	Average	Worst	Mean	Average	Worst	Mean	Average	Worst	Mean	Average	Worst	Mean
Pre-trained	91.7	46.8	71.1	91.7	46.8	71.1	90.6	50.1	75.5	90.6	50.1	75.5
ERM	89.3	69.4	80.2	88.6	67.2	80.0	95.7	77.4	87.8	96.1	82.2	89.7
GroupDRO	88.5	74.9	82.1	86.3	74.0	80.7	91.4	88.5	90.2	93.3	85.5	90.4
CPT	87.7	<b>75.2</b>	<b>83.9</b>	83.1	<b>78.9</b>	<b>81.2</b>	91.4	<b>89.4</b>	<b>90.5</b>	92.2	<b>89.2</b>	<b>91.5</b>

Model	Last layer ViT-B/32 393216			Prompting ViT-B/32 8192			Last layer ViT-L/14 786432			Prompting ViT-L/14 12288		
	Average	Worst	Mean	Average	Worst	Mean	Average	Worst	Mean	Average	Worst	Mean
Pretrained	90.1	49.0	72.2	90.1	49.0	72.2	89.4	36.1	83.9	89.4	36.1	83.9
ERM	94.7	73.5	85.2	94.0	76.0	85.7	96.6	85.8	91.8	96.8	83.1	91.6
GroupDRO	90.7	81.6	86.8	88.3	82.3	85.9	95.8	88.9	92.8	95.5	86.3	91.5
CPT	87.4	<b>86.3</b>	<b>87.4</b>	86.8	<b>85.2</b>	<b>87.5</b>	94.8	<b>90.7</b>	<b>92.9</b>	94.9	<b>90.0</b>	<b>92.6</b>

Similarly, Table 5 presents the scores of ERM, GroupDRO, and CPT on a wide range of CLIP backbones, including CLIP with ResNet101, ViT-B/16, ViT-B/32, ViT-L/14. Here we simply use the balanced version of CPT instead of hyperparameter tuning on  $c$ . Therefore, note that we do not try to beat GroupDRO on all metrics, but focus on investigating how our optimization procedure helps close the gap among groups. In summary, balancing the learning among groups results in large improvements in worst-group and mean accuracies for all backbones.

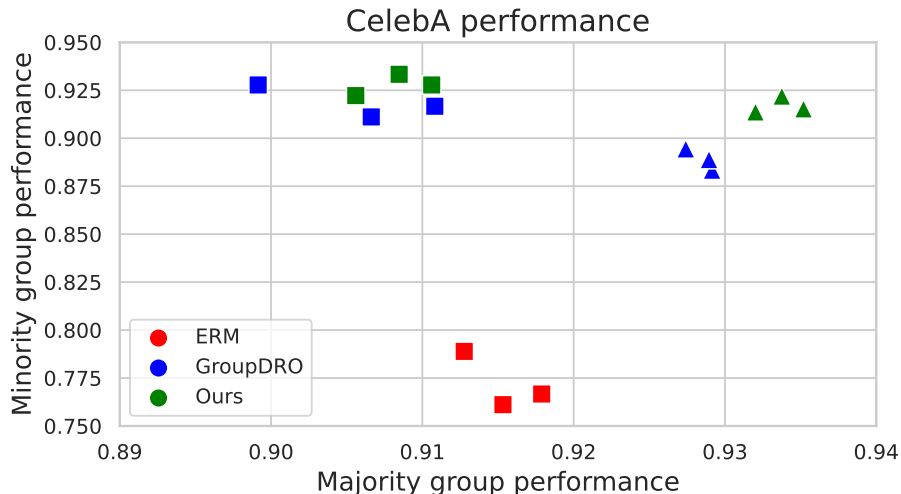


Figure 4: Performance of ResNet50 at: the last checkpoint used for evaluation (highest worst group accuracy on validation set), denoted by  $\triangle$ , and the checkpoint where the performance on the minority group is highest, denoted by  $\square$ . Results are obtained on three random seeds.

**Gap among group performance** Apart from Figure 1, we visualize the performance of each comparative method at its early stopping epoch and the point when it actually obtains the highest

score on the minority group in Figure 4. Those points collapse in the case of ERM since it does not have any balancing mechanism. Unsurprisingly, the gap between minority and majority performance of ERM is largest ( $> 10\%$ ) while this figure decreases for GroupDRO and CPT. It is true that GroupDRO can obtain a relatively high score on the minority group early in training, even on par with CPT. However, its majority group performance at this point has not converged yet ( $\approx 90.5\%$ ), and when converged, its performance on the minority group declines considerably ( $91\% \rightarrow 88\%$ ). By contrast, there is only a small difference in terms of minority performance for CPT at those points, allowing to have equally good performance across groups through training.

Table 6: Performance of the model after training for one epoch. Here, we simply adjust the optimization in favor of two minority groups to observe their improvement.

Group $g$ (size)	0 (44%)	1 (41%)	2 (14%)	3 (1%)	Worst	Avg	Mean
GroupDRO	92.0	92.5	91.5	86.1	86.1	92.08	89.4
CPT $c = (1, 1, 1, 1)$	<b>92.9</b>	<b>93.4</b>	92.8	91.7	<b>91.7</b>	<b>93.1</b>	92.7
CPT $c = (1, 1, 1, 2)$	92.0	91.1	93.1	<b>95.6</b>	91.1	91.9	93.0
CPT $c = (1, 1, 2, 1)$	91.2	91.8	<b>95.2</b>	95.0	91.2	92.0	<b>93.3</b>

**Effect of controlling vector** Table 6 presents the distribution of the CelebA dataset and the performance of GroupDRO and our proposed method with different values of the controlling vectors. We can see that setting  $c$  equal to the default value  $(1, 1, 1, 1)$  can perfectly balance the accuracy score across groups while GroupDRO encounters difficulty in fitting the minority one. Furthermore, by varying the value of  $c$ , we could observe different behavior of the model in each group. For example, the accuracy scores on two smaller groups (2&3) increase significantly, as a result of the loss magnitudes decrease when we put more weight on penalizing those two. With a tiny sacrifice on the performance of two majority groups, the model could gain considerable improvement in minority groups and the overall performance.

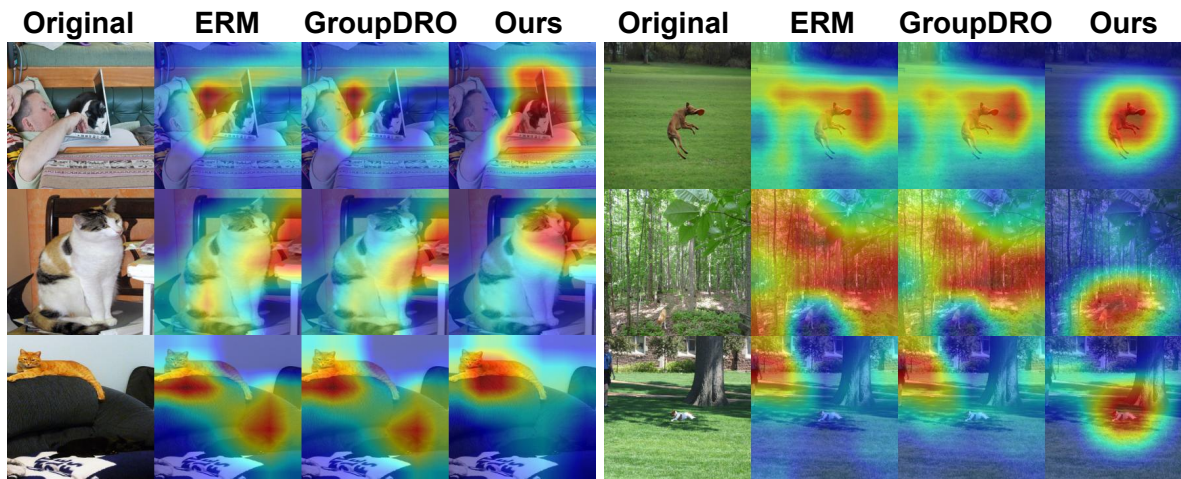


Figure 5: GradCAM of ResNet50 on in-domain samples.

**Saliency maps** We plot the saliency maps [70] produced when predicting the target attribute of in-domain images in Figure 5 and out-of-domain images in Figure 6. Pixels highlighted by warmer

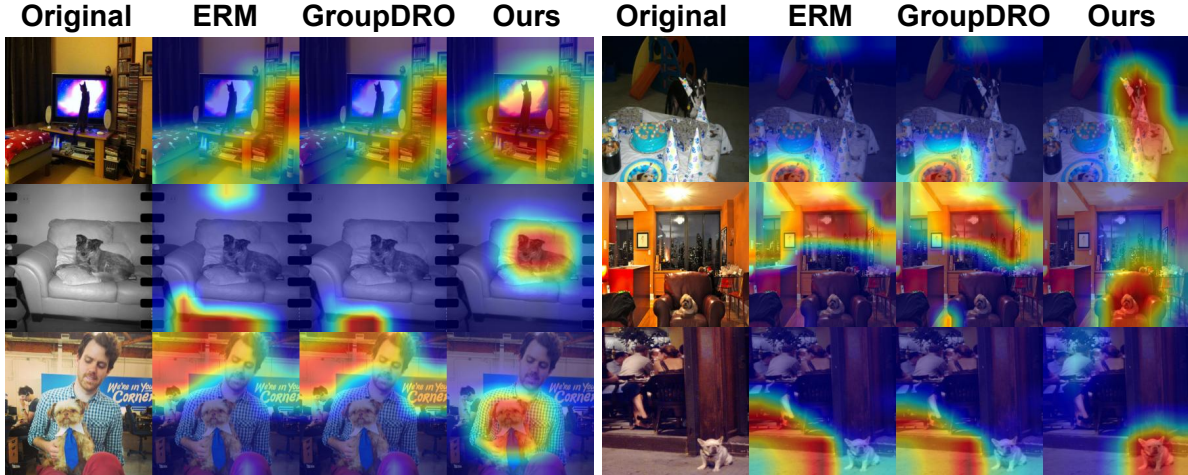


Figure 6: GradCAM of ResNet50 on OOD samples.

colors indicate higher contributions to the model predictions. Our proposed method can learn causal features rather than focusing on spurious background features when making predictions. Hence, balancing the learning among groups not only de-bias the classifier in-domain but also robustifies it in tackling distributional shifts.

## 6 Conclusion

In this paper, we propose Controllable Prompt Tuning, a novel training method that not only improves the performance across groups but also allows us to control the tradeoff between them. Our proposed method can effectively de-bias the training of different types of backbones and achieves state-of-the-art performance on benchmark datasets.

## References

- [1] S. Agarwal, G. Krueger, J. Clark, A. Radford, J. W. Kim, and M. Brundage. Evaluating clip: towards characterization of broader capabilities and downstream implications. *arXiv preprint arXiv:2108.02818*, 2021.
- [2] A. Aghajanyan, L. Zettlemoyer, and S. Gupta. Intrinsic dimensionality explains the effectiveness of language model fine-tuning. *arXiv preprint arXiv:2012.13255*, 2020.
- [3] F. Ahmed, Y. Bengio, H. Van Seijen, and A. Courville. Systematic generalisation with group invariant predictions. In *International Conference on Learning Representations*, 2020.
- [4] K. Ahuja, E. Caballero, D. Zhang, J.-C. Gagnon-Audet, Y. Bengio, I. Mitliagkas, and I. Rish. Invariance principle meets information bottleneck for out-of-distribution generalization. *Advances in Neural Information Processing Systems*, 34:3438–3450, 2021.
- [5] M. Andersen, J. Dahl, and L. Vandenberghe. Cvxopt: Convex optimization. *Astrophysics Source Code Library*, pages ascl-2008, 2020.
- [6] M. Arjovsky, L. Bottou, I. Gulrajani, and D. Lopez-Paz. Invariant risk minimization. *arXiv preprint arXiv:1907.02893*, 2019.
- [7] S. Ben-David, J. Blitzer, K. Crammer, A. Kulesza, F. Pereira, and J. W. Vaughan. A theory of learning from different domains. *Machine learning*, 79:151–175, 2010.
- [8] D. Berthelot, R. Roelofs, K. Sohn, N. Carlini, and A. Kurakin. Adamatch: A unified approach to semi-supervised learning and domain adaptation. In *International Conference on Learning Representations*, 2021.
- [9] A. Bissoto, E. Valle, and S. Avila. Debiasing skin lesion datasets and models? not so fast. In *Proceedings of the IEEE/CVF Conference on Computer Vision and Pattern Recognition Workshops*, pages 740–741, 2020.
- [10] A. P. Bradley. The use of the area under the roc curve in the evaluation of machine learning algorithms. *Pattern recognition*, 30(7):1145–1159, 1997.
- [11] T. Cai, R. Gao, J. Lee, and Q. Lei. A theory of label propagation for subpopulation shift. In *International Conference on Machine Learning*, pages 1170–1182. PMLR, 2021.
- [12] C.-F. R. Chen, Q. Fan, and R. Panda. Crossvit: Cross-attention multi-scale vision transformer for image classification. In *Proceedings of the IEEE/CVF international conference on computer vision*, pages 357–366, 2021.
- [13] S. Chen, C. Ge, Z. Tong, J. Wang, Y. Song, J. Wang, and P. Luo. Adaptformer: Adapting vision transformers for scalable visual recognition. *Advances in Neural Information Processing Systems*, 35: 16664–16678, 2022.
- [14] Y. Chen, E. Rosenfeld, M. Sellke, T. Ma, and A. Risteski. Iterative feature matching: Toward provable domain generalization with logarithmic environments. *Advances in Neural Information Processing Systems*, 35:1725–1736, 2022.
- [15] N. Codella, V. Rotemberg, P. Tschandl, M. E. Celebi, S. Dusza, D. Gutman, B. Helba, A. Kalloo, K. Liopyris, M. Marchetti, et al. Skin lesion analysis toward melanoma detection 2018: A challenge hosted by the international skin imaging collaboration (isic). *arXiv preprint arXiv:1902.03368*, 2019.
- [16] C. Cortes, Y. Mansour, and M. Mohri. Learning bounds for importance weighting. *Advances in neural information processing systems*, 23, 2010.



- [17] C. Cortes, M. Mohri, and A. Muñoz Medina. Adaptation algorithm and theory based on generalized discrepancy. In *Proceedings of the 21th ACM SIGKDD International Conference on Knowledge Discovery and Data Mining*, pages 169–178, 2015.
- [18] L. Dehdashtian, Sepehr Wang and V. Boddeti. Fairerclip: Debiasing zero-shot predictions of clip in rkhs. In *International Conference on Learning Representations*, 2024.
- [19] Y. Deng, Y. Yang, B. Mirzasoleiman, and Q. Gu. Robust learning with progressive data expansion against spurious correlation. *Advances in neural information processing systems*, 2023.
- [20] J.-A. Désidéri. Multiple-gradient descent algorithm (mgda) for multiobjective optimization. *Comptes Rendus Mathématique*, 350(5-6):313–318, 2012.
- [21] J. Devlin, M.-W. Chang, K. Lee, and K. Toutanova. Bert: Pre-training of deep bidirectional transformers for language understanding. *arXiv preprint arXiv:1810.04805*, 2018.
- [22] S. Diamond and S. Boyd. Cvxpy: A python-embedded modeling language for convex optimization. *The Journal of Machine Learning Research*, 17(1):2909–2913, 2016.
- [23] A. Dosovitskiy, L. Beyer, A. Kolesnikov, D. Weissenborn, X. Zhai, T. Unterthiner, M. Dehghani, M. Minderer, G. Heigold, S. Gelly, et al. An image is worth 16x16 words: Transformers for image recognition at scale. In *International Conference on Learning Representations*, 2020.
- [24] Y. Du, F. Wei, Z. Zhang, M. Shi, Y. Gao, and G. Li. Learning to prompt for open-vocabulary object detection with vision-language model. In *Proceedings of the IEEE/CVF Conference on Computer Vision and Pattern Recognition*, pages 14084–14093, 2022.
- [25] A. Edalati, M. Tahaei, I. Kobyzev, V. P. Nia, J. J. Clark, and M. Rezagholizadeh. Krona: Parameter efficient tuning with kronecker adapter. *arXiv preprint arXiv:2212.10650*, 2022.
- [26] A. Fan, E. Grave, and A. Joulin. Reducing transformer depth on demand with structured dropout. In *International Conference on Learning Representations*, 2019.
- [27] Y. Ganin, E. Ustinova, H. Ajakan, P. Germain, H. Larochelle, F. Laviolette, M. Marchand, and V. Lempitsky. Domain-adversarial training of neural networks. *The journal of machine learning research*, 17(1):2096–2030, 2016.
- [28] M. Gheini, X. Ren, and J. May. Cross-attention is all you need: Adapting pretrained transformers for machine translation. In *Proceedings of the 2021 Conference on Empirical Methods in Natural Language Processing*, pages 1754–1765, 2021.
- [29] S. S. Ghosal and Y. Li. Are vision transformers robust to spurious correlations? *International Journal of Computer Vision*, pages 1–21, 2023.
- [30] N. Gruver, M. A. Finzi, S. Qiu, and A. G. Wilson. Large language models are zero-shot time series forecasters. In *Thirty-seventh Conference on Neural Information Processing Systems*, 2023.
- [31] I. Gulrajani and D. Lopez-Paz. In search of lost domain generalization. In *International Conference on Learning Representations*, 2020.
- [32] D. Guo, A. Rush, and Y. Kim. Parameter-efficient transfer learning with diff pruning. In *Annual Meeting of the Association for Computational Linguistics*, 2021.
- [33] H. He, J. Cai, J. Zhang, D. Tao, and B. Zhuang. Sensitivity-aware visual parameter-efficient fine-tuning. In *Proceedings of the IEEE/CVF International Conference on Computer Vision*, pages 11825–11835, 2023.

- [34] J. He, C. Zhou, X. Ma, T. Berg-Kirkpatrick, and G. Neubig. Towards a unified view of parameter-efficient transfer learning. In *International Conference on Learning Representations*, 2021.
- [35] K. He, X. Zhang, S. Ren, and J. Sun. Deep residual learning for image recognition. In *Proceedings of the IEEE conference on computer vision and pattern recognition*, pages 770–778, 2016.
- [36] J. J. Heckman. Sample selection bias as a specification error. *Econometrica: Journal of the econometric society*, pages 153–161, 1979.
- [37] N. Houlsby, A. Giurgiu, S. Jastrzebski, B. Morrone, Q. De Laroussilhe, A. Gesmundo, M. Attariyan, and S. Gelly. Parameter-efficient transfer learning for nlp. In *International Conference on Machine Learning*, pages 2790–2799. PMLR, 2019.
- [38] E. J. Hu, P. Wallis, Z. Allen-Zhu, Y. Li, S. Wang, L. Wang, W. Chen, et al. Lora: Low-rank adaptation of large language models. In *International Conference on Learning Representations*, 2021.
- [39] W. Hu, G. Niu, I. Sato, and M. Sugiyama. Does distributionally robust supervised learning give robust classifiers? In *International Conference on Machine Learning*, pages 2029–2037. PMLR, 2018.
- [40] Q. Huang, X. Dong, D. Chen, W. Zhang, F. Wang, G. Hua, and N. Yu. Diversity-aware meta visual prompting. In *Proceedings of the IEEE/CVF Conference on Computer Vision and Pattern Recognition*, pages 10878–10887, 2023.
- [41] N. Kim, J. Kang, S. Ahn, J. Ok, and S. Kwak. Removing multiple biases through the lens of multi-task learning. *International Conference on Machine Learning*, 2023.
- [42] P. Kirichenko, P. Izmailov, and A. G. Wilson. Last layer re-training is sufficient for robustness to spurious correlations. In *The Eleventh International Conference on Learning Representations*, 2022.
- [43] A. Kolesnikov, L. Beyer, X. Zhai, J. Puigcerver, J. Yung, S. Gelly, and N. Houlsby. Big transfer (bit): General visual representation learning. In *Computer Vision—ECCV 2020: 16th European Conference, Glasgow, UK, August 23–28, 2020, Proceedings, Part V 16*, pages 491–507. Springer, 2020.
- [44] D. Krueger, E. Caballero, J.-H. Jacobsen, A. Zhang, J. Binas, D. Zhang, R. Le Priol, and A. Courville. Out-of-distribution generalization via risk extrapolation (rex). In *International Conference on Machine Learning*, pages 5815–5826. PMLR, 2021.
- [45] A. Kumar, T. Ma, P. Liang, and A. Raghunathan. Calibrated ensembles can mitigate accuracy tradeoffs under distribution shift. In *Uncertainty in Artificial Intelligence*, pages 1041–1051. PMLR, 2022.
- [46] Q. Lei, W. Hu, and J. Lee. Near-optimal linear regression under distribution shift. In *International Conference on Machine Learning*, pages 6164–6174. PMLR, 2021.
- [47] B. Lester, R. Al-Rfou, and N. Constant. The power of scale for parameter-efficient prompt tuning. In *Proceedings of the 2021 Conference on Empirical Methods in Natural Language Processing*, pages 3045–3059, 2021.
- [48] B. Li, Y. Hu, X. Nie, C. Han, X. Jiang, T. Guo, and L. Liu. Dropkey for vision transformer. In *Proceedings of the IEEE/CVF Conference on Computer Vision and Pattern Recognition*, pages 22700–22709, 2023.
- [49] S. Li, X. Jin, Y. Xuan, X. Zhou, W. Chen, Y.-X. Wang, and X. Yan. Enhancing the locality and breaking the memory bottleneck of transformer on time series forecasting. *Advances in neural information processing systems*, 32, 2019.
- [50] X. L. Li and P. Liang. Prefix-tuning: Optimizing continuous prompts for generation. In *Proceedings of the 59th Annual Meeting of the Association for Computational Linguistics*, pages 4582–4597, 2021.

- [51] V. Lialin, V. Deshpande, and A. Rumshisky. Scaling down to scale up: A guide to parameter-efficient fine-tuning. *arXiv preprint arXiv:2303.15647*, 2023.
- [52] W. Liang and J. Zou. Metashift: A dataset of datasets for evaluating contextual distribution shifts and training conflicts. In *International Conference on Learning Representations*, 2021.
- [53] E. Z. Liu, B. Haghgoo, A. S. Chen, A. Raghunathan, P. W. Koh, S. Sagawa, P. Liang, and C. Finn. Just train twice: Improving group robustness without training group information. In *International Conference on Machine Learning*, pages 6781–6792. PMLR, 2021.
- [54] L. Liu, Y. Li, Z. Kuang, J.-H. Xue, Y. Chen, W. Yang, Q. Liao, and W. Zhang. Towards impartial multi-task learning. In *International Conference on Learning Representations*, 2020.
- [55] Y. Liu, M. Ott, N. Goyal, J. Du, M. Joshi, D. Chen, O. Levy, M. Lewis, L. Zettlemoyer, and V. Stoyanov. Roberta: A robustly optimized bert pretraining approach. *arXiv preprint arXiv:1907.11692*, 2019.
- [56] Z. Liu, P. Luo, X. Wang, and X. Tang. Deep learning face attributes in the wild. In *Proceedings of International Conference on Computer Vision (ICCV)*, December 2015.
- [57] Z. Liu, H. Mao, C.-Y. Wu, C. Feichtenhofer, T. Darrell, and S. Xie. A convnet for the 2020s. In *Proceedings of the IEEE/CVF conference on computer vision and pattern recognition*, pages 11976–11986, 2022.
- [58] M. Long, Z. Cao, J. Wang, and M. I. Jordan. Conditional adversarial domain adaptation. *Advances in neural information processing systems*, 31, 2018.
- [59] T. Miyato, S.-i. Maeda, M. Koyama, and S. Ishii. Virtual adversarial training: a regularization method for supervised and semi-supervised learning. *IEEE transactions on pattern analysis and machine intelligence*, 41(8):1979–1993, 2018.
- [60] J. Nam, H. Cha, S. Ahn, J. Lee, and J. Shin. Learning from failure: De-biasing classifier from biased classifier. *Advances in Neural Information Processing Systems*, 33:20673–20684, 2020.
- [61] D. Oh, D. Lee, J. Byun, and B. Shin. Improving group robustness under noisy labels using predictive uncertainty. *arXiv preprint arXiv:2212.07026*, 2022.
- [62] A. Panahi, S. Saeedi, and T. Arodz. Shapeshifter: a parameter-efficient transformer using factorized reshaped matrices. *Advances in Neural Information Processing Systems*, 34:1337–1350, 2021.
- [63] H. Phan, T. Le, T. Phung, A. T. Bui, N. Ho, and D. Phung. Global-local regularization via distributional robustness. In *International Conference on Artificial Intelligence and Statistics*, pages 7644–7664. PMLR, 2023.
- [64] V. Piratla, P. Netrapalli, and S. Sarawagi. Focus on the common good: Group distributional robustness follows. In *International Conference on Learning Representations*, 2021.
- [65] S. Qiu, A. Potapczynski, P. Izmailov, and A. G. Wilson. Simple and fast group robustness by automatic feature reweighting. In *International Conference on Machine Learning*. PMLR, 2023.
- [66] A. Radford, J. W. Kim, C. Hallacy, A. Ramesh, G. Goh, S. Agarwal, G. Sastry, A. Askell, P. Mishkin, J. Clark, et al. Learning transferable visual models from natural language supervision. In *International conference on machine learning*, pages 8748–8763. PMLR, 2021.
- [67] A. Radford, J. W. Kim, T. Xu, G. Brockman, C. McLeavey, and I. Sutskever. Robust speech recognition via large-scale weak supervision. In *International Conference on Machine Learning*, pages 28492–28518. PMLR, 2023.

- [68] S. Sagawa, P. W. Koh, T. B. Hashimoto, and P. Liang. Distributionally robust neural networks. In *International Conference on Learning Representations*, 2019.
- [69] S. Sagawa, A. Raghunathan, P. W. Koh, and P. Liang. An investigation of why overparameterization exacerbates spurious correlations. In *International Conference on Machine Learning*, pages 8346–8356. PMLR, 2020.
- [70] R. R. Selvaraju, M. Cogswell, A. Das, R. Vedantam, D. Parikh, and D. Batra. Grad-cam: Visual explanations from deep networks via gradient-based localization. In *Proceedings of the IEEE international conference on computer vision*, pages 618–626, 2017.
- [71] Y. Shi, J. Seely, P. Torr, N. Siddharth, A. Hannun, N. Usunier, and G. Synnaeve. Gradient matching for domain generalization. In *International Conference on Learning Representations*, 2021.
- [72] H. Shimodaira. Improving predictive inference under covariate shift by weighting the log-likelihood function. *Journal of statistical planning and inference*, 90(2):227–244, 2000.
- [73] B. Sun, J. Feng, and K. Saenko. Correlation alignment for unsupervised domain adaptation. *Domain adaptation in computer vision applications*, pages 153–171, 2017.
- [74] Y.-L. Sung, J. Cho, and M. Bansal. VI-adapter: Parameter-efficient transfer learning for vision-and-language tasks. In *Proceedings of the IEEE/CVF Conference on Computer Vision and Pattern Recognition*, pages 5227–5237, 2022.
- [75] S. A. Taghanaki, K. Choi, A. H. Khasahmadi, and A. Goyal. Robust representation learning via perceptual similarity metrics. In *International Conference on Machine Learning*, pages 10043–10053. PMLR, 2021.
- [76] H. Touvron, T. Lavril, G. Izacard, X. Martinet, M.-A. Lachaux, T. Lacroix, B. Rozière, N. Goyal, E. Hambro, F. Azhar, et al. Llama: Open and efficient foundation language models. *arXiv preprint arXiv:2302.13971*, 2023.
- [77] A. Vaswani, N. Shazeer, N. Parmar, J. Uszkoreit, L. Jones, A. N. Gomez, Ł. Kaiser, and I. Polosukhin. Attention is all you need. *Advances in neural information processing systems*, 30, 2017.
- [78] C. Wah, S. Branson, P. Welinder, P. Perona, and S. Belongie. The caltech-ucsd birds-200-2011 dataset. 2011.
- [79] C. Wang, S. Chen, Y. Wu, Z. Zhang, L. Zhou, S. Liu, Z. Chen, Y. Liu, H. Wang, J. Li, et al. Neural codec language models are zero-shot text to speech synthesizers. *arXiv preprint arXiv:2301.02111*, 2023.
- [80] J. Wang, Y. Liu, and X. Wang. Are gender-neutral queries really gender-neutral? mitigating gender bias in image search. In *Proceedings of the 2021 Conference on Empirical Methods in Natural Language Processing*, pages 1995–2008, 2021.
- [81] M. Wortsman, G. Ilharco, S. Y. Gadre, R. Roelofs, R. Gontijo-Lopes, A. S. Morcos, H. Namkoong, A. Farhadi, Y. Carmon, S. Kornblith, et al. Model soups: averaging weights of multiple fine-tuned models improves accuracy without increasing inference time. In *International Conference on Machine Learning*, pages 23965–23998. PMLR, 2022.
- [82] S. Wu, M. Yuksekgonul, L. Zhang, and J. Zou. Discover and cure: Concept-aware mitigation of spurious correlation. *International Conference on Machine Learning*, 2023.
- [83] M. Xu, J. Zhang, B. Ni, T. Li, C. Wang, Q. Tian, and W. Zhang. Adversarial domain adaptation with domain mixup. In *Proceedings of the AAAI conference on artificial intelligence*, volume 34, pages 6502–6509, 2020.

- [84] S. Yang, Y. Dong, R. Ward, I. S. Dhillon, S. Sanghavi, and Q. Lei. Sample efficiency of data augmentation consistency regularization. In *International Conference on Artificial Intelligence and Statistics*, pages 3825–3853. PMLR, 2023.
- [85] Y. Yang, B. Nushi, H. Palangi, and B. Mirzasoleiman. Mitigating spurious correlations in multi-modal models during fine-tuning. *International Conference on Machine Learning*, 2023.
- [86] H. Yao, Y. Wang, S. Li, L. Zhang, W. Liang, J. Zou, and C. Finn. Improving out-of-distribution robustness via selective augmentation. In *International Conference on Machine Learning*, pages 25407–25437. PMLR, 2022.
- [87] E. B. Zaken, Y. Goldberg, and S. Ravfogel. Bitfit: Simple parameter-efficient fine-tuning for transformer-based masked language-models. In *Proceedings of the 60th Annual Meeting of the Association for Computational Linguistics (Volume 2: Short Papers)*, pages 1–9, 2022.
- [88] R. Zhai, C. Dan, J. Z. Kolter, and P. K. Ravikumar. Understanding why generalized reweighting does not improve over erm. In *The Eleventh International Conference on Learning Representations*, 2022.
- [89] M. Zhang and C. Ré. Contrastive adapters for foundation model group robustness. *Advances in Neural Information Processing Systems*, 35:21682–21697, 2022.
- [90] M. Zhang, N. S. Sohoni, H. R. Zhang, C. Finn, and C. Re. Correct-n-contrast: a contrastive approach for improving robustness to spurious correlations. In *International Conference on Machine Learning*, pages 26484–26516. PMLR, 2022.
- [91] B. Zhou, A. Lapedriza, A. Khosla, A. Oliva, and A. Torralba. Places: A 10 million image database for scene recognition. *IEEE transactions on pattern analysis and machine intelligence*, 40(6):1452–1464, 2017.
- [92] K. Zhou, J. Yang, C. C. Loy, and Z. Liu. Learning to prompt for vision-language models. *International Journal of Computer Vision*, 130(9):2337–2348, 2022.
- [93] B. Zhu, Y. Niu, Y. Han, Y. Wu, and H. Zhang. Prompt-aligned gradient for prompt tuning. In *Proceedings of the IEEE/CVF International Conference on Computer Vision*, pages 15659–15669, 2023.
- [94] J. Zhu, S. Lai, X. Chen, D. Wang, and H. Lu. Visual prompt multi-modal tracking. In *Proceedings of the IEEE/CVF Conference on Computer Vision and Pattern Recognition*, pages 9516–9526, 2023.
- [95] E. Zitzler and L. Thiele. Multiobjective evolutionary algorithms: a comparative case study and the strength pareto approach. *IEEE transactions on Evolutionary Computation*, 3(4):257–271, 1999.

# Supplement to “Controllable Prompt Tuning For Balancing Group Distributional Robustness”

Due to space constraints, some details were omitted from the main paper. We therefore include proof for Theorem 4.1 in the main paper (Appendix A) and more detailed experimental results (Appendix B) in this supplementary material.

## A Proof of Theorem 4.1

**Theorem 4.1.** *Assume that the loss function  $\ell$  is differentiable up to the first order with respect to  $\theta$ , then following*

$$d_{\text{ent}} := \sum_{i=1}^K \nabla \ell_i(\theta) \left[ p_i \log(p_i) - p_i \sum_{j=1}^K \log(p_j) p_j \right]$$

where  $p_i = \frac{e^{\ell_i(\theta)}}{\sum_{j=1}^K e^{\ell_j(\theta)}}$ , maximizes the objective  $\mathcal{L}_{\text{ent}}(\theta)$ :

$$\mathcal{L}_{\text{ent}}(\theta) = H(\text{softmax}(\vec{\mathcal{L}}(\theta))) = H\left(\text{softmax}\left(\left\{\mathbb{E}_{P_{g_k}}[\ell(f_\theta(x), y)]\right\}_{k=1}^K\right)\right)$$

**Proof:** For brevity of notations, we denote  $\mathbb{E}_{P_{g_i}}[\ell(f_\theta(x), y)]$  as  $\ell_i(\theta)$  and  $p_i = \frac{e^{\ell_i(\theta)}}{\sum_{j=1}^K e^{\ell_j(\theta)}}$ . The derivative of  $\mathcal{L}_{\text{ent}}$  with respect to  $\theta$  is computed as:

$$\begin{aligned} \nabla \mathcal{L}_{\text{ent}}(\theta) &= - \sum_{i=1}^K \left\{ \nabla p_i [\log(p_i) + 1] \right\} = - \sum_{i=1}^K \left\{ [\log(p_i) + 1] \nabla \frac{e^{\ell_i(\theta)}}{\sum_{j=1}^K e^{\ell_j(\theta)}} \right\} \\ &= - \sum_{i=1}^K \left\{ [\log(p_i) + 1] \frac{\sum_{j=1}^K e^{\ell_j(\theta)} e^{\ell_i(\theta)} \nabla \ell_i(\theta) - e^{\ell_i(\theta)} \sum_{j=1}^K e^{\ell_j(\theta)} \nabla \ell_j(\theta)}{(\sum_{j=1}^K e^{\ell_j(\theta)})^2} \right\} \\ &= - \frac{1}{(\sum_{j=1}^K e^{\ell_j(\theta)})^2} \sum_{i=1}^K \left\{ [\log(p_i) + 1] e^{\ell_i(\theta)} \sum_{j=1}^K e^{\ell_j(\theta)} (\nabla \ell_i(\theta) - \nabla \ell_j(\theta)) \right\} \\ &= - \frac{1}{(\sum_{j=1}^K e^{\ell_j(\theta)})^2} \sum_{i=1}^K \left[ \log(p_i) e^{\ell_i(\theta)} \sum_{j=1}^K e^{\ell_j(\theta)} (\nabla \ell_i(\theta) - \nabla \ell_j(\theta)) \right] \\ &= - \frac{1}{(\sum_{j=1}^K e^{\ell_j(\theta)})^2} \sum_{i=1}^K \nabla \ell_i(\theta) \left[ \log(p_i) e^{\ell_i(\theta)} \sum_{j=1}^K e^{\ell_j(\theta)} - e^{\ell_i(\theta)} \sum_{j=1}^K \log(p_j) e^{\ell_j(\theta)} \right] \\ &= \sum_{i=1}^K \nabla \ell_i(\theta) \left[ p_i \sum_{j=1}^K \log(p_j) p_j - p_i \log(p_i) \right] \end{aligned} \tag{8}$$

We conclude the proof. It is noteworthy that when the loss function  $\ell$  is positive, one can also simplify the computation by minimizing the following balancing function:

$$\mathcal{L}'_{\text{ent}}(\theta) := H\left(\left\{\frac{\mathbb{E}_{P_{g_i}}[\ell(f_\theta(x), y)]}{\sum_{j=1}^K \mathbb{E}_{P_{g_j}}[\ell(f_\theta(x), y)]}\right\}_{i=1}^K\right)$$

Eliminating the exponential term and denoting  $q_i = \frac{\ell_i(\theta)}{\sum_{j=1}^K \ell_j(\theta)}$ , the gradient direction of the entropy term is given by:

$$\begin{aligned} \nabla \mathcal{L}'_{ent}(\theta) &= \sum_{i=1}^K \{ \nabla q_i [\log(q_i) + 1] \} \\ &= \sum_{i=1}^K \left\{ \frac{[\sum_{j=1}^K \ell_j(\theta)] \nabla \ell_i(\theta) - \ell_i(\theta) [\sum_{j=1}^K \nabla \ell_j(\theta)]}{[\sum_{j=1}^K \ell_j(\theta)]^2} [\log(q_i) + 1] \right\} \\ &\propto \sum_{i=1}^K \nabla \ell_i(\theta) \left\{ \log(q_i) \left[ \sum_{j=1}^K \ell_j(\theta) \right] - \sum_{j=1}^K \log(q_j) \ell_j(\theta) \right\} \end{aligned}$$

## B Experiment details and additional empirical results

In this section, we first describe the datasets and models used in Appendix B.1 along with the detailed training configuration for our method, then provide additional results for the experiment in Appendix B.2. Example images and data statistics are presented in Table 8, 9, 10 and 11.

### B.1 Implementation details

**Hyper-parameter** We mainly examine the proposed method on ResNet50 [35], ViT B/16 [23] and different variants of OpenAI’s CLIP<sup>1</sup> model. The hyperparameters selected for each experiment are given in Table 7. Unless stated otherwise, results of baselines are taken from original papers and [19, 82, 64, 90, 41], which provide standard evaluation protocols for different backbones and datasets. Performance of ERM and GroupDRO [68] at different amount of training data and their training curves are obtained from the released codebase of GroupDRO<sup>2</sup> using their provided commands.

Dataset	Architecture	Learning Rate	Weight Decay	Batch Size	# Epochs	Prompt length
Waterbirds	ViT B/16	0.1	0.001	64	100	10
Waterbirds	Last layers CLIP-RN50	0.003	0.01	32	100	-
Waterbirds	Prompt CLIP-RN50	0.03	0.01	32	100	16
Waterbirds	Last layer CLIP-ViT-L/14	0.01	0.01	32	100	-
Waterbirds	Prompt CLIP-ViT-L/14	0.001	0.01	32	100	16
CelebA	ViT B/16	0.01	0.001	128	100	10
MetaShift	ResNet50	0.003	0.01	16	100	-
MetaShift	ViT B/16	0.01	0.1	16	100	5
ISIC	ViT B/16	0.003	0.01	16	100	5

Table 7: Hyperparameter for different experiments throughout our paper. We report the hyperparameters selected for our proposed method after performing grid-search.

**Classifier design** While we train a classification head from scratch for ResNet50 or ViT, CLIP allows us to utilize its meaningful multimodality embeddings as a zero-shot classifier. In particular, given an image embedding  $\mathbf{e}_i$  and a text class embedding  $\mathbf{e}_t^k$  for some class index  $k \in \{1, 2, \dots, \mathbf{N}_c\}$ ,

<sup>1</sup><https://github.com/openai/CLIP>

<sup>2</sup>[https://github.com/kohpangwei/group\\_DRO](https://github.com/kohpangwei/group_DRO)

where  $N_c$  is the number of categories. The probability of the given image belonging to  $k$ -th class is computed as:

$$p(y = k | \mathbf{e}_i) = \frac{\exp(\langle \mathbf{e}_i, \mathbf{e}_t^k \rangle / \tau)}{\sum_{j=1}^{N_c} \exp(\langle \mathbf{e}_i, \mathbf{e}_t^j \rangle / \tau)}$$

where  $\langle \cdot, \cdot \rangle$  denotes the cosine similarity and  $\tau$  is the temperature parameter.

**Dataset statistics** We evaluate CPT on Waterbirds [68] (Table 8), CelebA [56] (Table 9), MetaShift [52] (Table 10) and ISIC [15] (Table 11), following previous work [68, 19, 82]. While the objective of those image classification tasks is predicting the categories of input images, those target attributes are often correlated well with spurious features (please refer to each table for detailed descriptions of spurious features and group partitions for each dataset).





Image				
Group	0	1	2	3
Label	0 (landbird)	0 (landbird)	1 (waterbird)	1 (waterbird)
Spurious feature	0 (land)	1 (water)	0 (land)	1 (water)
Description	landbird on land	landbird on water	waterbird on land	waterbird on water
# Train data	3,498(73%)	184(4%)	56(1%)	1,057(22%)
# Val data	467	466	133	133
# Test data	2,255	2,255	642	642

Table 8: Example images of Waterbirds [68].





Image				
Group	0	1	2	3
Label	0 (non-blond)	0 (non-blond)	1 (blond)	1 (blond)
Spurious feature	0 (woman)	1 (man)	0 (woman)	1 (man)
Description	non-blond woman	non-blond man	blond woman	blond man
# Train data	71,629(44%)	66,874(41%)	22,880(14%)	1,387(1%)
# Val data	8,535	8,276	2,874	182
# Test data	9,767	7,535	2,480	180

Table 9: Example images of CelebA [56].









Image						
Group	0	1	2	3	4	5
Label	0 (cat)	0 (cat)	1(dog)	1 (dog)	0 (cat)	1 (dog)
Spurious feature	0 (sofa)	1 (bed)	2 (bench)	3 (bike)	4 (shelf)	4 (shelf)
# Train data	231	380	145	367	-	-
# Val data (OOD)	-	-	-	-	34	47
# Test data	-	-	-	-	201	259

Table 10: Example images of MetaShift [52].

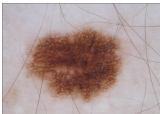
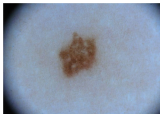
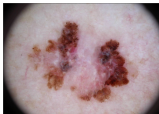
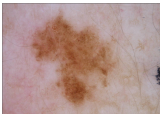
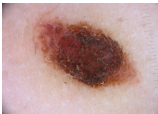
Image				...		
Label	0 (benign)	0 (benign)	1 (malignant)	...	0 (benign)	1 (malignant)
Spurious feature	hair	dark corner	gel bubbles	...	ink	ruler
# Train data:				1,826		
# Val data:				154		
# Test data:				618		

Table 11: Example images of ISIC [15].

## B.2 Additional experiments

**Prompt length** Thanks to the design of the prompting component, the computational burden during training is modest: only a small portion of the model parameters are updated through back-propagation. Here, we vary the value of prompt length  $L$  to observe its effect on the model performance in Table 12. Results of ERM, GroupDRO, the second-best method in this dataset DFR [42] and a recent baseline in this line of research PDE [19] are also included for a general comparison. While increasing the prompt length can improve the performance of the model, we find that just pretending one token per transformer layer ( $L = 1$ ) can outperform the second-best method that requires  $\times 2200$  more trainable parameters via better training. Last, it is noteworthy to highlight that  $L = 16$  can help CPT match the average accuracy score of ERM in this scenario, which demonstrates the large modeling capacity of our proposed method.

Table 12: Ablation results for different prompt length  $N$  on ViT B/16 on Waterbirds.

$N$	1	2	4	8	10	16	ERM	GroupDRO	PDE	DFR
Worst	92.9 $\pm$ 0.8	93.3 $\pm$ 0.9	93.5 $\pm$ 0.6	93.8 $\pm$ 0.5	93.5 $\pm$ 0.4	<b>93.9</b> $\pm$ 0.7	70.0 $\pm$ 2.3	86.7 $\pm$ 0.6	90.3 $\pm$ 0.3	92.9 $\pm$ 0.2
Average	95.8 $\pm$ 0.9	95.9 $\pm$ 0.9	96.4 $\pm$ 0.1	96.5 $\pm$ 0.0	96.3 $\pm$ 0.1	<b>97.1</b> $\pm$ 0.3	<b>97.1</b> $\pm$ 0.1	93.2 $\pm$ 0.5	92.4 $\pm$ 0.8	94.2 $\pm$ 0.2
Mean	94.9 $\pm$ 0.8	95.2 $\pm$ 0.0	95.6 $\pm$ 0.4	<b>96.0</b> $\pm$ 0.8	95.7 $\pm$ 0.2	95.7 $\pm$ 0.3	N/A	N/A	N/A	N/A
# Params	10754	19970	38402	75266	93698	148994	23512130	23512130	23512130	23512130

**Performance at different number of training samples** In order to comprehensively assess the performance of our proposed model, we conduct a series of experiments to analyze its behavior across varying sizes of training data. Those experiments were designed to investigate the impact of data size on the model performance of comparative methods. We keep group ratios preserved

while subsampling a part of the training data. The x-axis of Figure 7 denotes the percentages of the Waterbirds and CelebA training set used in each sub-experiment. It can be seen that CPT is better than GroupDRO or ERM in lower data regimes. Remarkably, by using 20% and 10% data, our proposed method can still outperform other baselines when using the full training set.

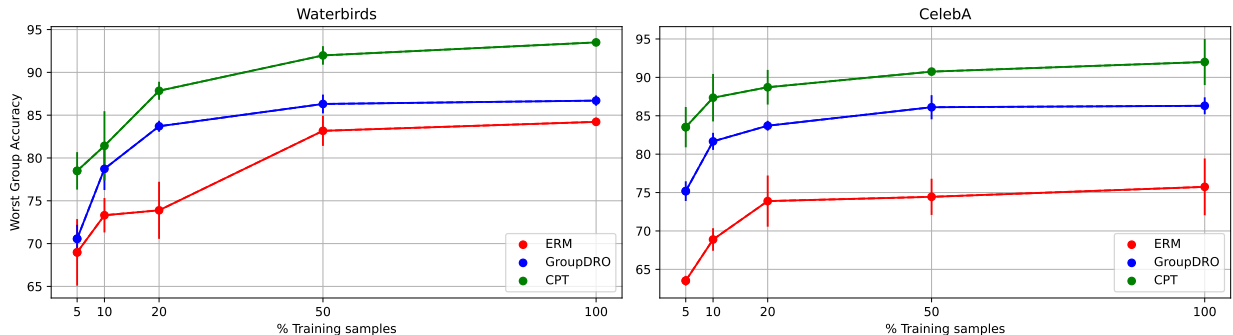


Figure 7: Data Efficiency on Waterbirds (left) and CelebA (right). Error bars correspond to standard deviations over three trials.

Similarly, we run the above experiment but replace the main backbone with CLIP-RN50 and plot the performance of different baselines. Note that we freeze both image and text encoders and employ prompt tuning on their text encoder only. The text prompt used for training CLIP models is:

*“a type of bird, a photo of a waterbird/landbird”*

While the pretrained CLIP model obtains 90.9% average accuracy on Waterbirds (Table 2 in the main paper), it severely suffers from unintended bias when attaining only 44.9% worst-group accuracy. This motivates the need for debiasing methods to remove such bias and mitigate the reliance on spurious features when making predictions of foundation models. Figure 8 shows that while using more data can help enhance the pre-trained CLIP model better for all methods, CPT obtains the best worst group accuracy for every amount of data and surpasses the current state-of-the-art method [85].

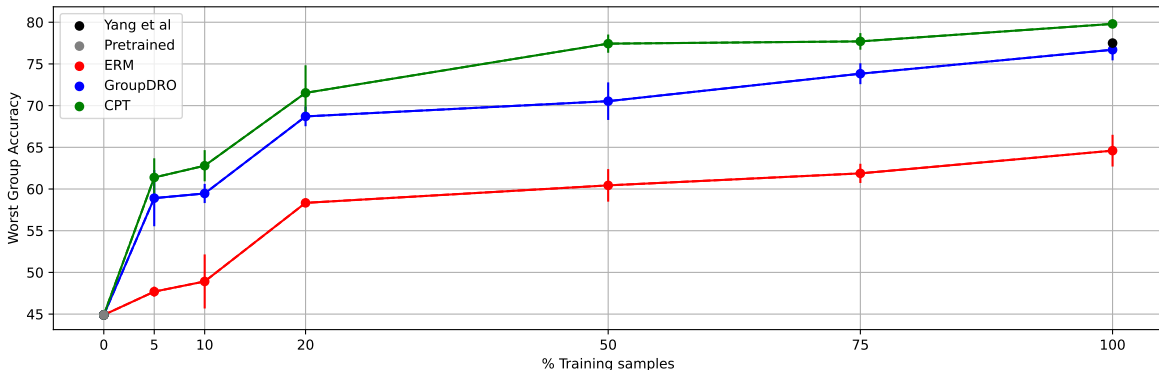


Figure 8: Data Efficiency of CLIP-RN50. CPT with 75% data can outperform the current state-of-the-art method for debiasing CLIP [85] which uses  $\times 1800$  trainable parameters.

**Running time** Figure 9 summarizes the total runtime and the time for solving the linear programming problem on each epoch. The introduction of the optimization (7) in the main paper leads to a small overhead in terms of training time. However, this small sacrifice significantly boosts the performance of different backbones, especially for CLIP and prompt-based models. For example, prompt-tuning on CLIP variants takes only 0.3 second per epoch since it does not have to update the entire network or even the classification head.

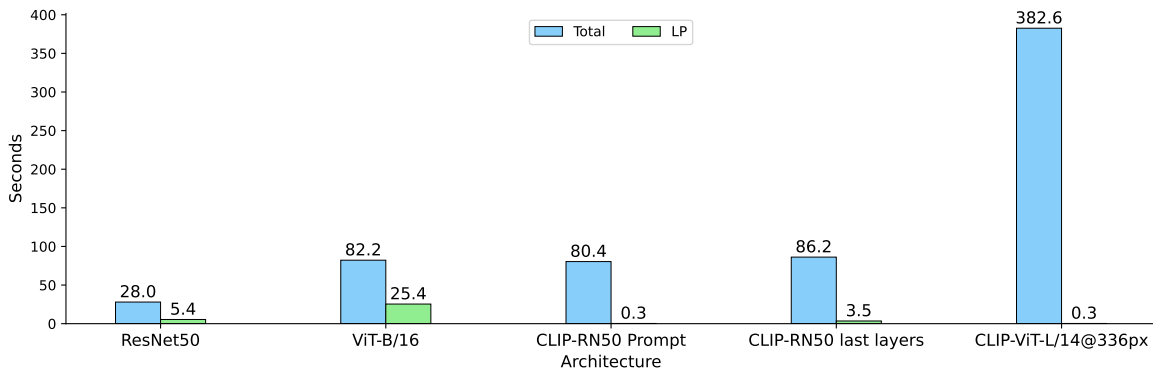


Figure 9: Total running time and the time for solving the linear programming (LP) problem on epoch with Intel(R) Xeon(R) Platinum 8358 CPU @ 2.60GHz and NVIDIA A100-SXM4-80GB GPU. Results are averaged over 5 epochs.

**Debiasing ViT** For the experiment of debiasing Vision Transformer, we compare CPT against different ViT and Big Transfer (BiT) models introduced in [43, 29]. More detailed results are given in Table 13, from which we can see that CPT not only obtains the best worst-group accuracy score but also performs on par with the second-best method in terms of average

Table 13: Comparison of different backbones on Waterbirds

Model	Average Acc.	Worst-Group Acc.	# Params
BiT-M-R50x1	92.05 $\pm$ 0.05	75.10 $\pm$ 0.62	23.5M
BiT-M-R50x3	94.90 $\pm$ 0.05	80.51 $\pm$ 1.02	211M
BiT-M-R101x1	94.05 $\pm$ 0.07	77.50 $\pm$ 0.50	42.5M
ViT-Ti/16	89.50 $\pm$ 0.05	71.65 $\pm$ 0.16	5.6M
ViT-S/16	96.30 $\pm$ 0.51	85.45 $\pm$ 1.16	21.8M
ViT-B/16	96.75 $\pm$ 0.05	89.30 $\pm$ 1.95	86.1M
CPT	96.33 $\pm$ 0.15	<b>93.51</b> $\pm$ 0.36	<b>94k</b>

accuracy while using much fewer parameters. Note that other models scale up the resolution to  $384 \times 384$  while CPT keeps using the  $224 \times 224$  resolution.

**Saliency maps** We here provide more GradCAM visual explanations for ERM, GroupDRO and CPT on Waterbirds in Figure 10 and CelebA Figure 11. From those images, CPT shows its ability to identify causal features for making predictions, compared to ERM and GroupDRO. Hence, our balancing mechanism helps prevent the model from learning spurious features that occur frequently during training.

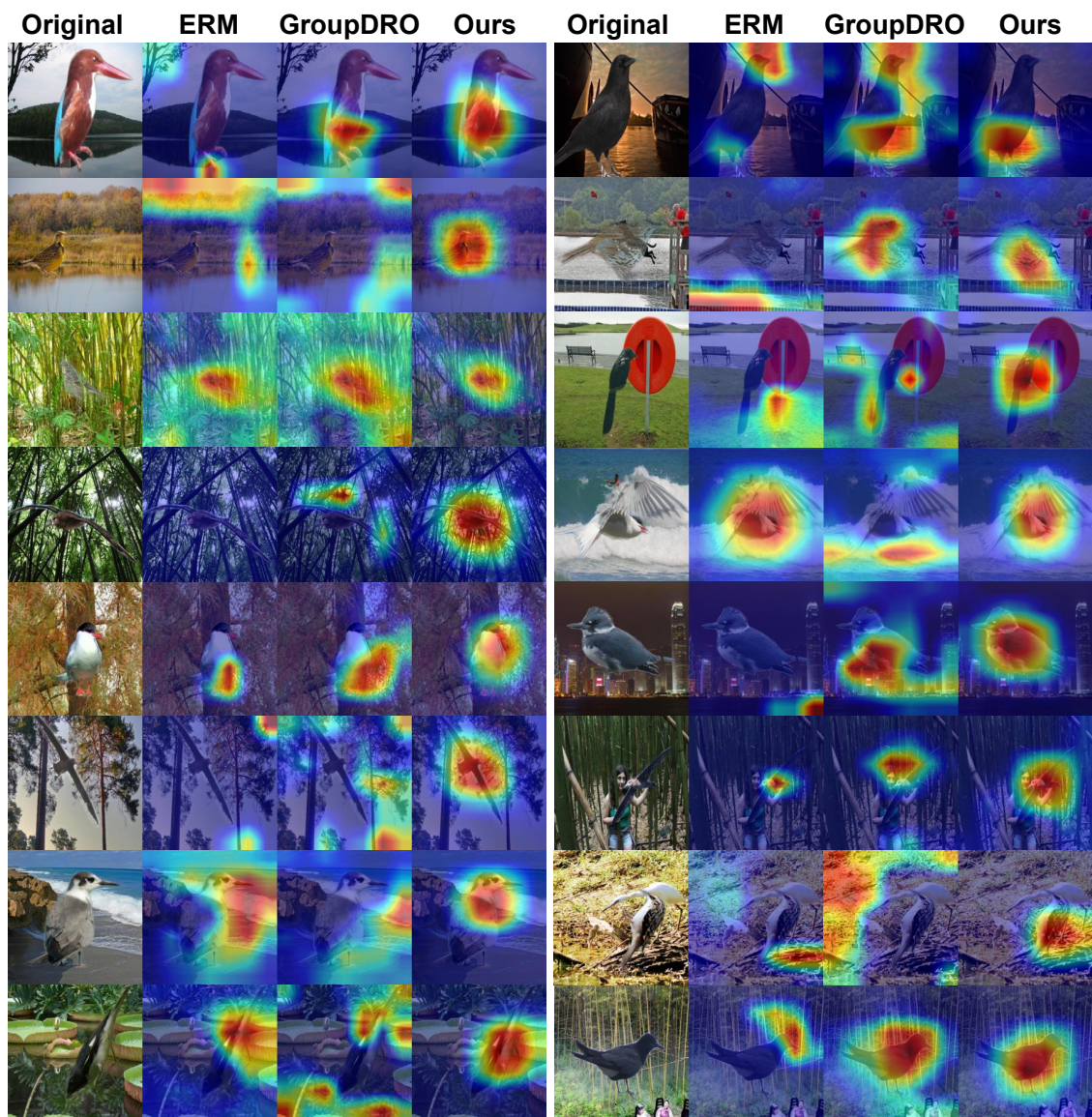


Figure 10: Waterbirds GradCAM.

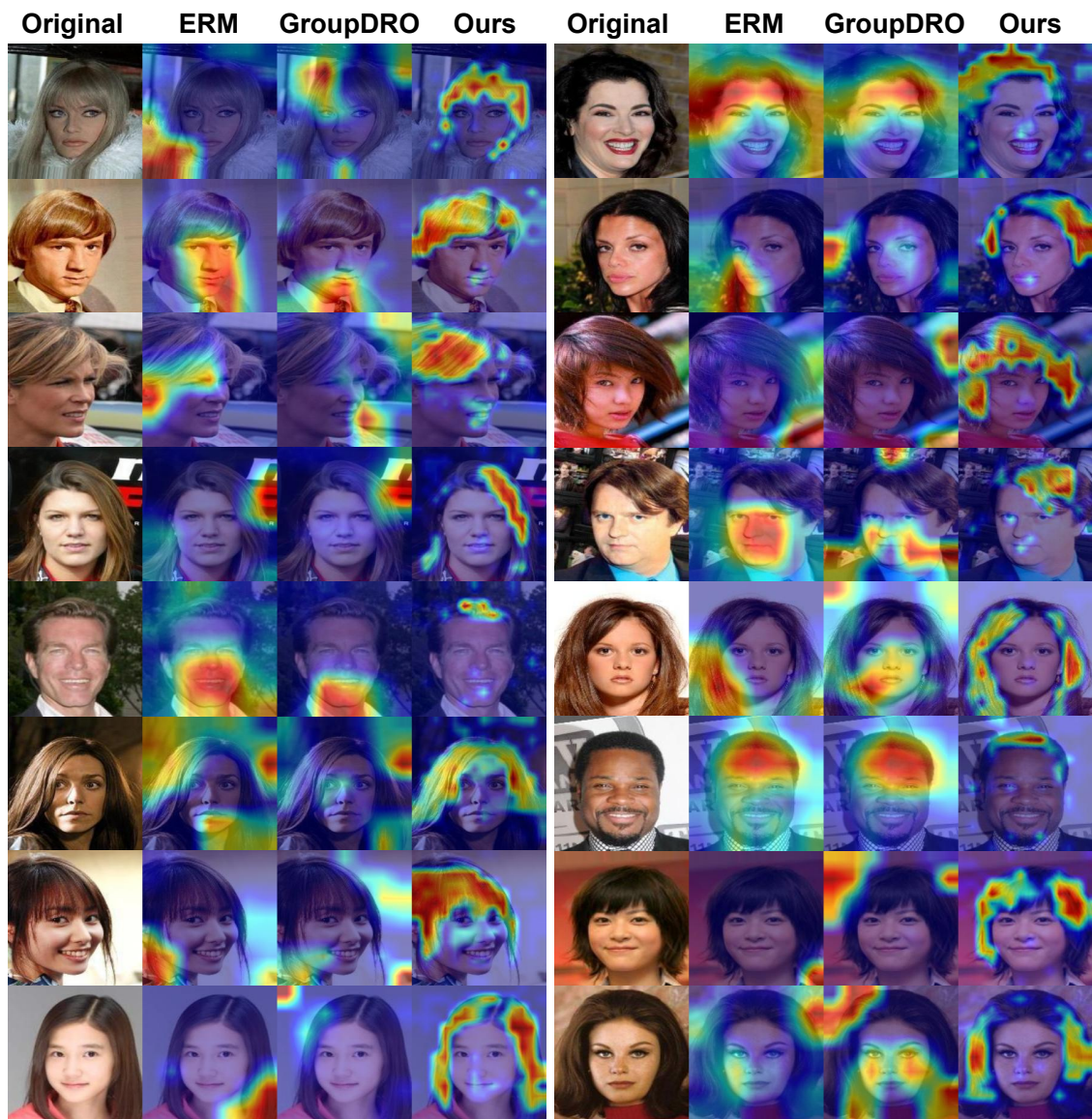


Figure 11: CelebA GradCAM.